

Article

Effects of Sodium Gluconate on the Fluidity and Setting Time of Phosphorus Gypsum-Based Self-Leveling

Xuepeng Shen ¹, Hao Ding ¹, Zhichun Chen ², Ying Li ³, Wenxuan An ³, Aili Chen ⁴, Dongyi Lei ^{3,*} , Ying Fang ^{1,*} and Dongxu Li ^{1,*}

¹ College of Materials Science and Engineering, Nanjing Tech University, Nanjing 210009, China; 202161103080@njtech.edu.cn (X.S.); 202161203249@njtech.edu.cn (H.D.)

² Technical Supervision and Research Center of the Building Materials Industry, Beijing 100024, China; czc910@163.com

³ School of Civil Engineering, Qingdao University of Technology, Qingdao 266033, China; 13346092644@163.com (W.A.)

⁴ Nanjing Kunchang New Material Co., Nanjing 210049, China; 15189837773@163.com

* Correspondence: leidongyi@qut.edu.cn (D.L.); powderfang@163.com (Y.F.); dongxuli@njtech.edu.cn (D.L.)

Abstract: To comprehensively utilize industrial by-products of gypsum while reducing the consumption of natural river sand, this experiment was conducted to prepare gypsum-based sandless self-leveling (PGSL) materials by using phosphorus-building gypsum (PBG) and portland cement (PC) as gelling raw materials with the addition of polycarboxylate superplasticizer (PCE), cellulose ethers (CE), and retarders. However, employing phosphogypsum as the source material results in a significant 30 min fluidity loss in the gypsum-based self-leveling system. Therefore, to enhance the flow characteristics of gypsum self-leveling, sodium gluconate was chosen for usage in this research. The impact of single and compound mixing of protein-based retarder (PR) and sodium gluconate (SG) on gypsum-based sandless self-leveling materials was evaluated in terms of heat of hydration analysis, pore structure, fluidity, strength, and setting time. According to the experimental findings, it was possible to considerably decrease the fluidity loss of gypsum-based sandless self-leveling materials, postpone the setting time, boost strength, and enhance pore structure when combined with 0.4% SG and 0.03% PR.

Keywords: gypsum self-leveling; fluidity loss; hydration; $\text{CaSO}_4\cdot 2\text{H}_2\text{O}$; phosphorus impurities



Citation: Shen, X.; Ding, H.; Chen, Z.; Li, Y.; An, W.; Chen, A.; Lei, D.; Fang, Y.; Li, D. Effects of Sodium Gluconate on the Fluidity and Setting Time of Phosphorus Gypsum-Based Self-Leveling. *Buildings* **2024**, *14*, 89. <https://doi.org/10.3390/buildings14010089>

Academic Editor: Xiaoyong Wang

Received: 3 December 2023

Revised: 22 December 2023

Accepted: 26 December 2023

Published: 28 December 2023



Copyright: © 2023 by the authors. Licensee MDPI, Basel, Switzerland. This article is an open access article distributed under the terms and conditions of the Creative Commons Attribution (CC BY) license (<https://creativecommons.org/licenses/by/4.0/>).

1. Introduction

Phosphogypsum is a solid waste obtained in the process of phosphorus fertilizer production, and its main component is $\text{CaSO}_4\cdot 2\text{H}_2\text{O}$. Subsequently, beta-hemihydrate gypsum ($\beta\text{-CaSO}_4\cdot 0.5\text{H}_2\text{O}$) and alpha-hemihydrate gypsum ($\alpha\text{-CaSO}_4\cdot 0.5\text{H}_2\text{O}$) can be obtained using different calcination methods. According to the various qualities of phosphate ore, 1 ton can yield about 4–6 tons of phosphogypsum [1,2]. China is a significant producer of phosphogypsum production; the annual growth rate of phosphogypsum is about 70 million metric tons, of which the comprehensive utilization rate is only 15 percent. Due to the incomplete understanding of phosphogypsum in the early days, a lot of phosphogypsum was piled up near rivers and oceans, and the accumulation of a large amount of phosphogypsum caused significant damage to the surrounding environment, such as polluting the nearby soil and making the water source eutrophic, etc. [3–5]. Therefore, during the period of rapid national development, it is of great significance to seek new ways of complete utilization of phosphogypsum to improve the comprehensive utilization rate of phosphogypsum and to promote the construction of socialist modernization and civilization. Gypsum building materials prepared with phosphogypsum as the primary cementitious material can greatly reduce the amount of cement, reduce carbon dioxide emissions, are less harmful to the environment, and are a new type of green building

material [6–8]. Among them, gypsum-based self-leveling mortar is a kind of dry powder material specially used for indoor leveling. It performs better in terms of acoustic isolation, thermal insulation, and moisture absorption, and provides micro-expansion after hydration to counteract the contraction produced by the hydration of cement components [9].

In traditional gypsum-based self-leveling materials, natural river sand is usually added as an aggregate filler. Still, due to the continuous development of society and urbanization, the consumption of wild river sand has significantly increased. The water–sand balance of the river has been altered by excessive sand mining, which has an impact on the river’s stability and ecosystem and seriously threatens the safety of the river channel, the flood control levees, and the arable land [10–12], and most of the mechanism sand has an angular, rough surface, which, although it will improve the strength a little, is not conducive to mobility; we need to add too much water to improve mobility, which will again be unfavorable to the strength [13], and the actual construction of gypsum self-leveling is mostly done by machine pumping. The addition of sand will increase the gravity of self-leveling, which is not conducive to the efficiency of pumping. Consequently, it is imperative to prepare gypsum-based self-leveling materials without sand. In order to design gypsum-based self-leveling mortar, Zhi et al. [9] used high-strength gypsum to prepare gypsum self-leveling mortar and to research the impact of chemical admixtures on the mortar’s setting time, liquidity, and mechanical qualities.

The first step in improving phosphogypsum utilization is to reduce the impact of phosphogypsum impurities on the gypsum. Among them, the biggest influences on the performance of phosphogypsum are phosphorus impurities and fluorine impurities. Among phosphorus impurities, phosphorus impurities mainly exist in the form of H_3PO_4 , $\text{Ca}_3(\text{PO}_4)_2$, $\text{FePO}_4 \cdot 2\text{H}_2\text{O}$, HPO_4^{2-} , $\text{CaHPO}_4 \cdot 2\text{H}_2\text{O}$, H_2PO_4^- , and $\text{Ca}(\text{H}_2\text{PO}_4)_2 \cdot \text{H}_2\text{O}$ [14,15]. Among them, soluble phosphorus has a more significant impact on the performance of gypsum, and the presence of soluble P_2O_5 significantly hinders the hydration, coagulation, and hardening processes of phosphorus gypsum and reduces the strength of its hardened body. In an acidic environment, soluble phosphorus mainly exists as H_3PO_4 , H_2PO_4^- , and HPO_4^{2-} , while in an alkaline environment, phosphorus impurities mainly exist as PO_4^{3-} , which can easily combine with metal cations in the system to form inert insoluble phosphorus salts, which have much less effect on gypsum than soluble salts. Taken together, the magnitude of the impact on gypsum properties is $\text{H}_3\text{PO}_4 > \text{H}_2\text{PO}_4^- > \text{HPO}_4^{2-} > \text{PO}_4^{3-}$ [16]. At present, the gypsum-based self-leveling prepared with phosphogypsum is mostly $\beta\text{-CaSO}_4 \cdot 0.5\text{H}_2\text{O}$, which has an irregular crystal structure compared with $\alpha\text{-CaSO}_4 \cdot 0.5\text{H}_2\text{O}$, and the gypsum-based self-leveling obtained from it has a lower strength and a larger loss of fluidity. Therefore, solving the excessive fluidity loss of phosphorus gypsum-based self-leveling has become a complex problem. Wang et al. [17] added calcium sulphoaluminate cement and three kinds of ground slag to gypsum self-leveling and found that two types of ground slag with small particle sizes can control the fluidity loss of 30 min to less than 3 mm. In addition to the slag and the cement in the appropriate ratio, it can also ensure a higher 1 d strength. Sliva et al. [18] added a highly effective polycarboxylate superplasticizer (PCE) to gypsum-based self-leveling at a suitable solubility and discovered that, despite the fact that the setting time does not adhere to the standard, the mechanical properties of gypsum self-leveling and the flow properties can be relatively good in the water–cement ratio of 0.5, glue–sand ratio of 1:0.5, and PCE of 1%.

Sodium gluconate is an organic compound with numerous industrial applications [19]. It can be used as a highly effective superplast and a highly effective retarder agent in the concrete industry, as well as an efficient chelating agent in construction, textile printing and dyeing, metal surface treatment, water treatment, cleaning of steel surfaces, and cleaning of glass bottles. Ma et al. [19] added SG to cement concrete and found that it increased the 3 d and 28 d compressive strengths, delayed setting time, and increased the fluidity of cement mortar. To enhance the performance of polycarboxylate-type (PCE) superplasticizers synergistically, Ren et al. [20] added SG to cement pastes. By grafting PCE side chains, they discovered that including SG improved PCE’s fluidity and flow

retention. A red-mud-based blended alkali-activated cement was given SG by Lin et al. [21]. They discovered that it enhanced the fluidity of the paste and considerably slowed the pace of hydration. Numerous studies have indicated that SG greatly improves cement flow properties [19–21], but its reflection in gypsum is still relatively scarce. Typically, gypsum-based sandless self-leveling materials prepared from phosphogypsum usually have a significant loss of flow properties after 30 min. Gypsum self-leveling is usually pumped by machine in practical use, so the requirement for flow properties is very high. In this paper, SG and PR were used to improve this property of the material, and it was found that the addition of SG greatly improved the flowability after 30 min, improved the strength and other physical properties, evaluated the hydration process, porosity, and pore structure of the material, and finally successfully prepared a gypsum-based sandless self-leveling material with excellent properties.

2. Materials and Methods

2.1. Raw Materials

Guizhou Kailai Green Building Materials Co., Guizhou 551199, China, provided the phosphorus-containing building gypsum for this paper. It is grayish-white in appearance. Table 1 lists the fundamental physical characteristics, and Table 2 lists the chemical makeup.

Table 1. PBG’s fundamental physical characteristics.

Water to Gypsum Ratio (%)	Setting Time (s)		Flexural Strength (MPa)		Compressive Strength (MPa)	
	Initial	Final	2 h	3 d-Dry	2 h	3 d-Dry
66	120	270	3.1	3.7	6.9	15.3

Table 2. The percentages of PBG and PC’s chemical makeup.

Component	SO ₃	CaO	SiO ₂	P ₂ O ₅	Al ₂ O ₃	Fe ₂ O ₃	Na ₂ O	K ₂ O	Loss
PBG	50.51	36.62	2.09	0.98	0.52	0.39	0.023	0.11	8.44
PC	2.31	57.67	20.69	0.41	6.3	5.74	0.1	0.52	9.93

The phase composition of PBG is depicted in Figure 1a, which demonstrates that CaSO₄·0.5H₂O is the primary constituent of this PBG. According to GB/T 36141-2018 [22], the amount of CaSO₄·0.5H₂O was calculated to be 87.57 wt%. Gypsum powder’s apparent morphology as seen by scanning electron microscopy is depicted in Figure 1c, where it can be seen that the powder mostly takes the shape of a plate and contains a lot of irregularly shaped particles. Phosphorus, fluoride, alkali metal salt, and other organic contaminants were adsorbed onto the surface of the particles. The PBG particle size distribution is depicted in Figure 1b; the average particle size is 33.898 μm.

Anhui Conch Cement Co. manufactures this cement kind, which is PC 42.5. Purchased from Jiangsu Zhaojia Building Material Technology Co., Suzhou 215000, China, the superplasticizer is a polycarboxylate superplasticizer (PCE). Organosilicon defoamer (OD), a product of Jiangsu Zhaojia Building Materials Technology Co., Suzhou 215000, China, is an antifoam agent. Hydroxypropyl methylcellulose (CE), the ingredient in cellulose ether, can be purchased from Shenzhen Tongzhouda Co., Shenzhen 518000, China. Retarder was acquired from Jiangsu Zhaojia Building Material Technology Co., Suzhou 215000, China, and is a polypeptide-bonded polymer (PR). SG (industrial grade) was purchased from Shandong Kaixiang Biotechnology Co., Shandong 262300, China.

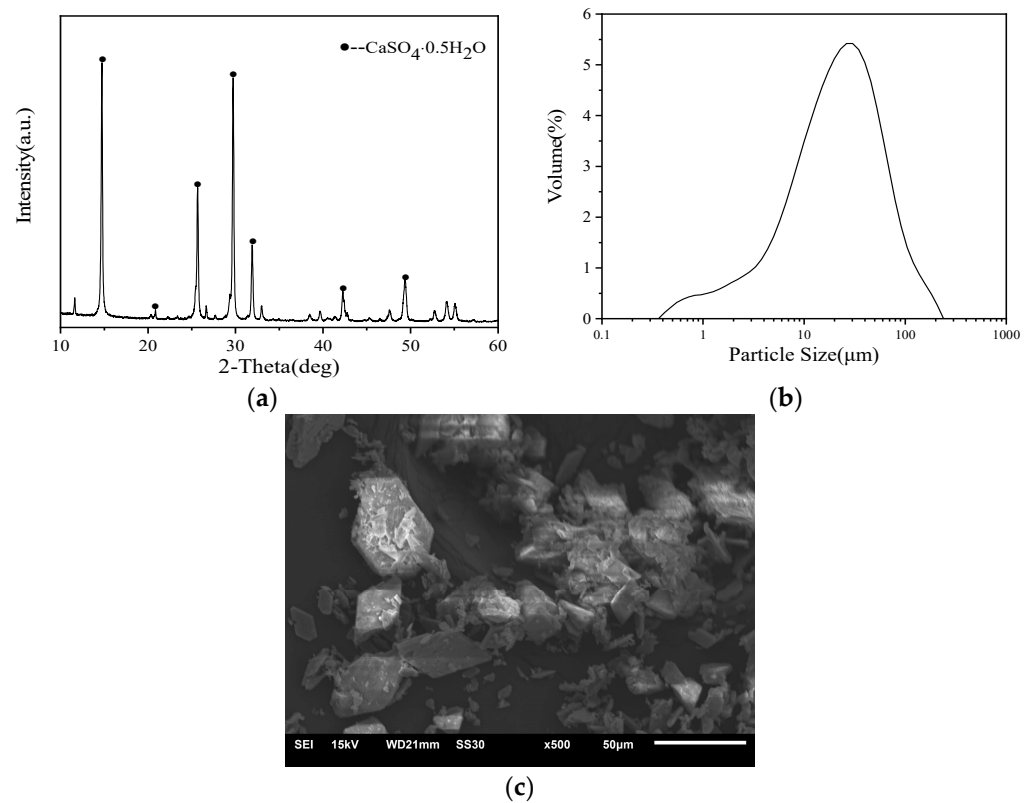


Figure 1. Characterization of PBG: (a) XRD; (b) particle size distribution; and (c) SEM image.

2.2. Sample Preparation Process

Table 3 lists the specific proportion design used in this paper: gypsum-based sandless self-leveling material admixture dosage based on the weight of dry powder, of which PCE is 0.15%, PR is 0.03%, OD is 0.1%, and CE is 0.03%, and the ratio of water to the amount of dry powder is 0.40.

Table 3. Mix proportions for the PGSL.

No.	PBG (wt%)	PC (wt%)	SG (wt%)	PR (wt%)
P0	95	5	0.04	0
K0	95	5	0	0.03
K1	95	5	0.01	0.03
K2	95	5	0.02	0.03
K3	95	5	0.03	0.03
K4	95	5	0.04	0.03
K5	95	5	0.05	0.03
K6	95	5	0.06	0.03

PBG was used as the primary cementitious material, and a small amount of PC was added to adjust the pH value of the system. The mass fraction of gypsum was 95%, and the mass fraction of cement was 5%. According to the test method stipulated in JC/T 1023-2021 [23], weighing was carried out by the proportions in Table 3, first stirring slowly for 60 s, scraping down the pan wall and mixing blade unevenly within 30 s, then stirring quickly for 60 s, and then stirring fast for 15 s after 60 s of static stopping until no bubbles were produced, to get the homogeneous slurry. Then, immediately loaded into a 40 mm by 40 mm by 160 mm cement sand test mold, the slurry is filled with a scraper to scrape flat. Then put the test mold into the constant temperature and humidity maintenance box (relative humidity $\geq 90\%$, temperature $20\text{ }^{\circ}\text{C} \pm 1\text{ }^{\circ}\text{C}$) for molding and maintenance. A flow chart for the specific preparation of gypsum self-leveling can be seen in Figure 2.

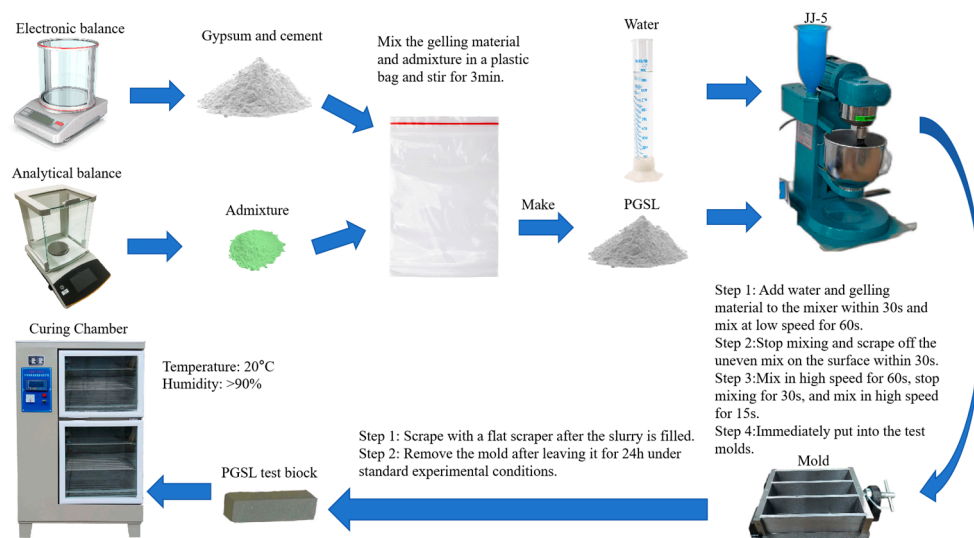


Figure 2. Flow chart for the preparation of gypsum-based self-leveling.

2.3. Test Method

2.3.1. Physical Properties

(1) Fluidity

According to the building materials industry standard JC/T 1023-2021 test, the test mold's fluidity was placed horizontally in the middle of the test plate, the slurry was stirred uniformly and poured into it, excess slurry was scraped off of the test mold's upper mouth, the test mold was raised vertically by 50–100 mm within 2 s, held for 10–15 s, and the slurry was allowed to flow freely for 4 min. Then the diameter of two vertical directions of the cake was measured, and the arithmetic average was taken to be accurate to 1 mm. The result was the initial fluidity. After 4 min of free flow of the slurry, measure the diameter of the two vertical directions of the cake, take the arithmetic mean value, accurate to 1 mm, and obtain the initial degree of flow. The above slurry was in the mixing bowl to stand for 30 min, mix for 30 s, and then poured into the two flowability test molds, respectively, to measure its flow; the 30 min fluidity was the arithmetic average of the above two fluidities.

(2) Setting time and strength

The sample's setting time was evaluated using the Chinese national standard GB/T 17669.4-1999 [24]. The sample's strength was evaluated in accordance with GB/T 17669.3-1999 [25]. The samples were dried at 40 °C in an oven until they reached a constant weight after curing for a predetermined amount of time. They were then loaded at a rate of 2.4 kN/s into an automatic compressive strength tester (Model AEC-201, Wuxi Alicon Instrument and Equipment Co., Wuxi 214000, China.) to test the samples' flexural and compressive strengths. The samples' flexural and compressive strengths were calculated.

(3) Rate of size change

The size change rate of the sample was tested according to the building materials industry standard JC/T 985-2005 [26]. After the sample was molded, it was placed under standard experimental conditions for (24 ± 0.5) h, the test direction was marked, and the length of the sample was tested in the marked direction within 30 min after demoulding, which was the initial length (L_0). Cured under standard experimental conditions for $28 \text{ d} \pm 8 \text{ h}$, the length of the specimen was tested according to the indicated direction, i.e., the length after natural drying (L_t). The rate of dimensional change of the sample was calculated using the following Equation (1)

$$\varepsilon = \frac{L_t - L_0}{L - L_d} \times 100\% \quad (1)$$

where ε is the rate of dimensional change. L_0 is the length of the specimen 24 h after moulding (mm), L_t is the length of the sample drying naturally for 28 d (mm), L is the length of the sample 160 mm, and L_d is the sum of the lengths of the two shrinkage heads buried in the slurry and the value of 20 ± 2 (mm). The average value of three specimens was taken as the final shrinkage rate.

2.3.2. Microscopic Properties

(1) Hydration process

A TAM AIR 8 calorimeter was used to measure the heat of the PGSL hydration process at 25 °C for 72 h, where the water–gel ratio was 0.4, in order to assess the exothermic behavior of the substance.

(2) Phase composition (XRD)

The physical structure of the samples was examined using an X-ray diffractometer (D/max-2200PC) from Rigaku, Japan, with a scanning rate of 10°/min and a scanning range of 10° to 80°.

(3) Pore structure analysis (MIP)

The pore structure of the PGSL was examined using a Poremaster GT-6.0 (Kantar Instruments USA, Inc., Lake Zurich, FL, USA), Quantum Chrome Mercuric Pressure instrument (MIP) from the United States after small sections of the center part had been removed and submerged in alcohol, dried, and evaluated. The measured pore size during the test ranged from 7.0 nm to 200.0 μm , while the incursion pressure ranged from 1.0 to 30,000.0 psi.

(4) Micromorphology (SEM)

After smashing the PGSL, the middle part was taken and glued to the conductive tape and gold plated. The samples were tested for microscopic properties using a scanning electron microscope (IT-300) from JEOL, Japan.

3. Results

3.1. Effect of SG on the Setting Time of PGSL

The impact of SG on the samples' setting time is depicted in Figure 3. It has been discovered that adding either SG or PR will lengthen the PGSL setting time. P0's beginning and final setting times are just 34 min and 43 min, which is considerably too little time and well below what is actually needed. In contrast, K0's initial and final setting times are 134 min and 216 min, respectively, which can accommodate the needs of actual use. Additionally, the initial setting time and final setting time of PGSL both significantly increase when PR and SG are combined, with the effect on the final setting time being more pronounced. This indicates that the time between the initial setting time and the final setting time is also growing. This is because PR itself has a large number of amino and carboxyl groups that chelate with Ca^{2+} in the slurry, on the one hand, reducing the Ca^{2+} solubility of the system; on the other hand, these chelates cover the surface of gypsum crystals, changing the way dihydrate gypsum ($\text{CaSO}_4 \cdot 2\text{H}_2\text{O}$) crystals grow, thus delaying the nucleation process of the nucleus, which is then manifested as a prolongation of gypsum coagulation time [27]. Additionally, SG contains a variety of functional groups, like carboxyl and hydroxyl groups, that can react with Ca^{2+} in the system to form chelates. Because PR has a higher adsorption capacity than SG, its influence on retardation is more pronounced. When these two retarders are compounded, the adsorption capacity of the whole system on Ca^{2+} is greatly strengthened, and the macroscopic performance of PGSL is prolonged in the coagulation time.

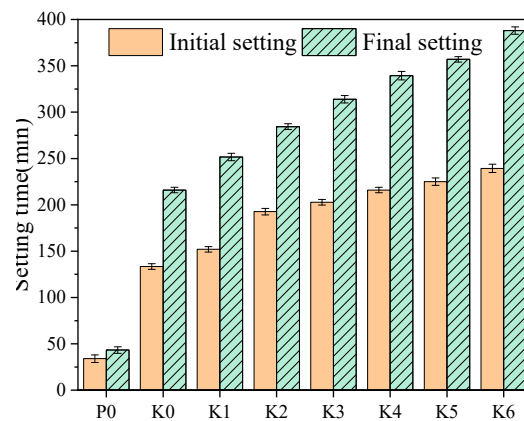


Figure 3. Effect of SG on the setting time of the samples.

3.2. Effect of SG on the Fluidity of PGSL

The impact of SG on the samples' fluidity is depicted in Figure 4. As depicted in Figure 4, the early fluidity of PGSL is specifically enhanced with an increase in SG dose. This is due to the addition of SG to a certain extent to promote the dispersion of the PCE [28], which assists in water reduction. So, when sodium gluconate is added, the initial fluidity of the self-leveling increases. In addition, the 30 min fluidity of P0 and K0 is almost lost. P0 is because if only SG is added, the retarding effect is relatively limited, and the 30 min is close to the initial setting time, so there is no fluidity after 30 min, whereas K0 is due to the impurities of the PBG itself, such as phosphoric acid, fluorine, and phosphoric acid impurities. The 30 min fluidity of PGSL is significantly improved after the compounding of PR and SG, which is increased to 120 mm at the addition of 0.01%. With the increase of SG, the fluidity increased, and the fluidity loss before and after 30 min is only 2 mm at the addition of 0.06%. Therefore, the addition of SG significantly improves the fluidity of PGSL.

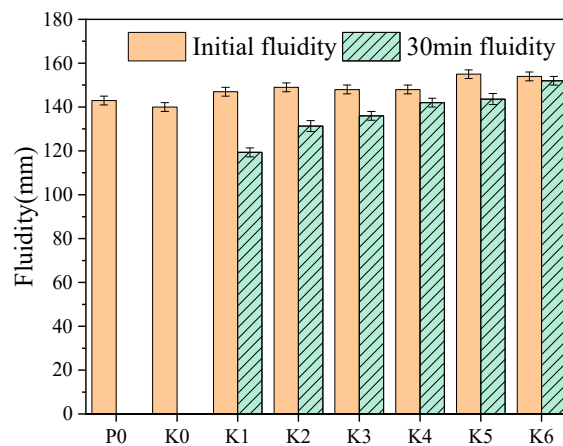


Figure 4. Effect of SG on the fluidity of the samples.

On the one hand, gypsum is acidic, while the addition of SG is weakly alkaline. After the addition of cement and the role of the system together to regulate the pH, gypsum in the alkaline environment, the H_3PO_4 transformed into $H_2PO_4^-$, HPO_4^{2-} , and PO_4^{3-} , which have a much smaller impact on the performance of gypsum than H_3PO_4 [14–16]. However, many active functional groups, such as the carboxyl and hydroxyl groups in SG, react with free calcium ions to produce insoluble calcium salts, which precipitate on the surface of C_3A and $CaSO_4 \cdot 0.5H_2O$ to form a calcium salt encapsulation layer. This effectively slows down the hydration rate of PGSL, in addition to SG incorporation at a level of less than 0.1%, which can promote the dispersion of PCE [28]. Under the combined

effect of these three factors, the 30 min fluidity of PGSL is significantly improved by adding SG.

3.3. Effect of SG on the Mechanical Strength of PGSL

Figure 5 shows the effect of SG incorporation on the flexural and compressive strengths of PGSL. It can be seen that the late strength of K0 doped with PR alone is higher, while the early strength of P0 doped with SG alone is higher. The 1 d and 3 d flexural strengths of PGSL showed a trend of decreasing in the first rise and decreasing in the second rise with the increase of SG doping, while the 28 d strength showed a trend of increasing in the first rise and dropping in the second rise, with the flexural strength of K2 at 28 d, which is enhanced by 31.37%, showing the most significant increase. Gypsum self-leveling is combined with SG and PR, and it is discovered that the 28 d compressive strength of the self-leveling showed a rising and falling pattern with the rise of SG dosage, with the strength of K4 increasing most noticeably, with a 6.38% increase. The strength of K5 and K6 decreased more particularly, which may be due to the addition of excessive SG, which seriously slowed down gypsum's hydration degree and thus reduced the strength. Comprehensively, when the SG dosage reaches 0.04%, although it will reduce the early strength, it still meets the early strength requirements of JC/T 1023-2021, and it can improve a certain amount of late strength.

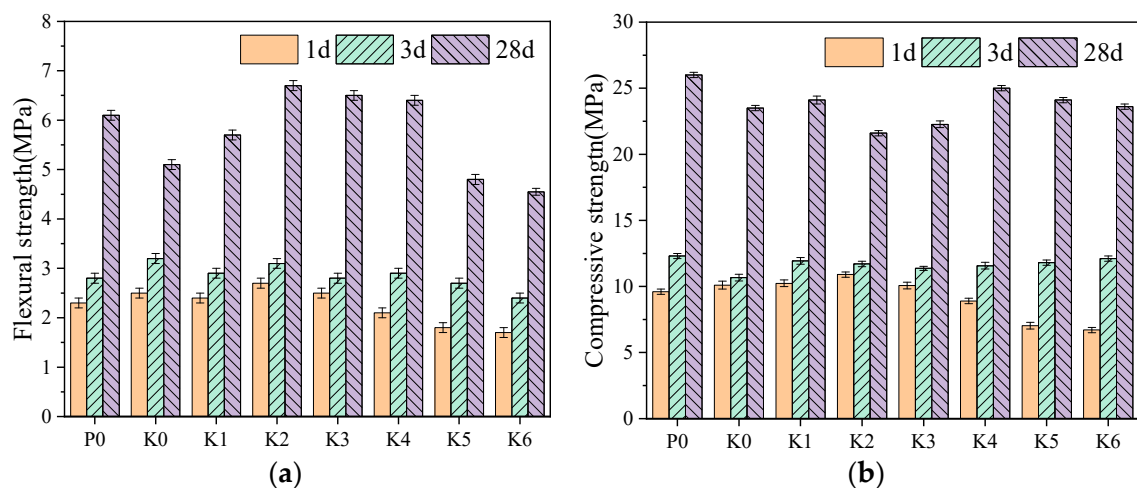


Figure 5. Effect of SG on the (a) Flexural strength and (b) Compressive strength of the samples.

3.4. Rate of Size Change at 28 d

Figure 6 shows the effect of SG incorporation on the rate of size change of PGSL. From the graph, it can be seen that the rate of dimensional change of PGSL shows a trend of decreasing and then increasing with the addition of SG, with the lowest rate of size change when the SG doping is 0.03% and 0.04%, i.e., K3 and K4. Since construction gypsum's theoretical water demand is 18.6% of its weight [29], the overall PGSL in this experiment demonstrated a phenomenon of shrinking. The amount of water given to PGSL in the experiment was significantly greater than the amount of water that was theoretically needed for it. As a result, during PGSL's subsequent hydration process, the excess water separated as water vapor, which caused PGSL to shrink. In this experiment, some PCs were added, which might lead to micro-expansion in the later hydration stage, but it was not enough to make up for the shrinkage caused by the gypsum. As a result, the PGSL as a whole exhibits a propensity for contraction. During subsequent hydration, this separates extra water from the PGSL as water vapor.

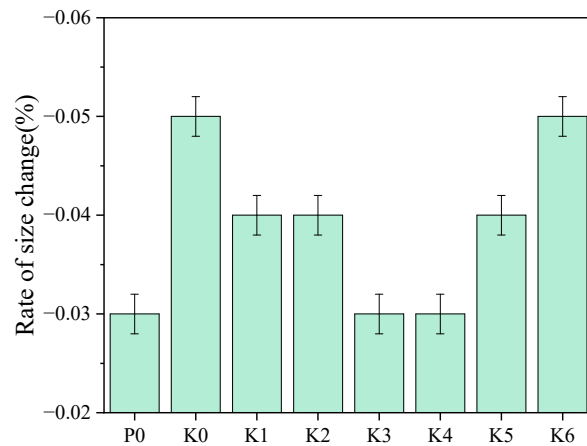


Figure 6. Effect of SG on the size change rate of the samples.

3.5. Heat of Hydration

The exothermic trend of hydration for various samples is shown in Figure 7. It is clear from the first peak in Figure 7a that the hydration of PBG occurs in stages. The $\text{CaSO}_4 \cdot 0.5\text{H}_2\text{O}$ is dissolved in water and comes into contact with it in the first step, releasing the heat of hydration. The rate of this stage is rather fast, and it is difficult to notice. Then, in the second stage, with the continual dissolution of $\text{CaSO}_4 \cdot 0.5\text{H}_2\text{O}$ in water and the accompanying precipitation of $\text{CaSO}_4 \cdot 2\text{H}_2\text{O}$, the exothermic heat increases further. The stage of the accelerated phase is marked by a sharp temperature increase. The deceleration period represents the third stage, which occurs as the exothermic rate falls [30,31]. The heat of hydration diagrams show that the induction duration of gypsum lengthens with the addition of SG and that the peak of the heat of hydration of gypsum is delayed with an increase in the dose of SG. The addition of SG prolongs the coagulation time of PGSL. A second peak can be seen in the heat of the hydration curve as a result of the expansion of 5% PC in this experimental system. This is because PC has two exothermic peaks that correspond to the accelerated and decelerated phases of hydration, where the first peak coincides with the exothermic peak of gypsum. The inclusion of SG delays the second peak. The addition of SG hinders the hydration of C_3A and retards the hydration process of C_3A , which results in the delay of the second exothermic peak [19,32,33].

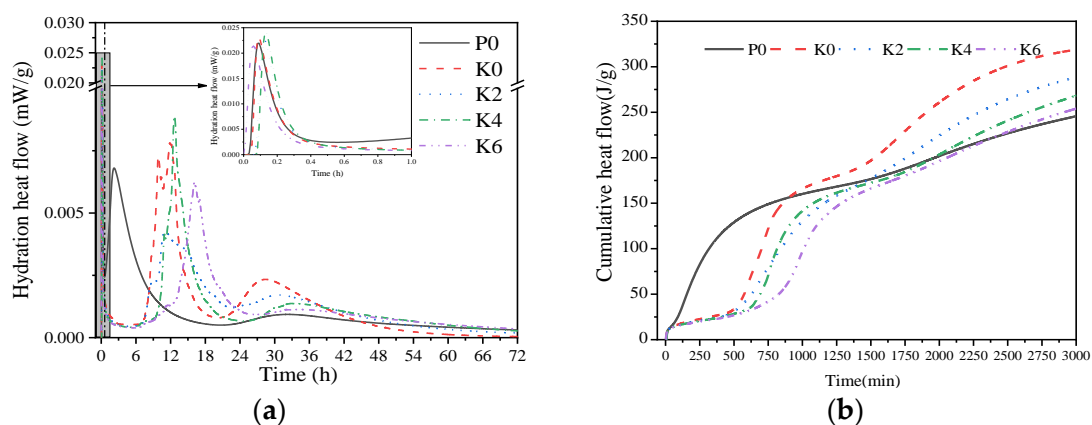


Figure 7. (a) Heat of hydration and (b) Cumulative heat release of the samples.

From Figure 6b, it can be seen that the early exothermic heat of hydration is less in K0 relative to P0, but the total exothermic heat is higher. The higher early cumulative exothermic heat in P0 may be because the single doping of SG does not significantly affect the hydration process of C_3A , which makes the early exothermic heat of PC and gypsum cumulative. Thus, the early cumulative exothermic heat in P0 is higher. Co-doping with

SG has a weakening effect on the cumulative exotherm of PGSL. According to general rules, the higher the heat of hydration, the greater the degree of hydration reaction, and the greater the fluidity loss [17,34]. However, as shown in Figure 6b, the heat of hydration decreases with an increase in SG, and the corresponding fluidity loss also decreases, which is consistent with Figure 4.

3.6. XRD

The XRD patterns of PGSL at 1 d, 3 d, and 28 d are displayed in Figure 8. The majority of the $\text{CaSO}_4 \cdot 0.5\text{H}_2\text{O}$ has been hydrated into $\text{CaSO}_4 \cdot 2\text{H}_2\text{O}$ after 1 d of hydration, as shown in Figure 7a. However, some of the $\text{CaSO}_4 \cdot 0.5\text{H}_2\text{O}$ remains unhydrated and has noticeable diffraction peaks. As shown in Figure 6a, the diffraction peaks of $\text{CaSO}_4 \cdot 2\text{H}_2\text{O}$ became more pronounced when SG was added, indicating that SG can postpone $\text{CaSO}_4 \cdot 2\text{H}_2\text{O}$'s hydration. The XRD spectra of the PGSL hydrated for 3 d are displayed in Figure 7b. It is evident that at this point, $\text{CaSO}_4 \cdot 2\text{H}_2\text{O}$ has completely hydrated to become $\text{CaSO}_4 \cdot 2\text{H}_2\text{O}$, with the unique peak of $\text{CaSO}_4 \cdot 2\text{H}_2\text{O}$ from K0 being more significant than that of P0. However, the $\text{CaSO}_4 \cdot 2\text{H}_2\text{O}$ diffraction peaks are most effective at a 0.02% SG dosage when these two retarders are combined, while the distinctive peak is at its weakest at a 0.04% SG dosage. When the hydration process reaches 28 d, the diffraction peaks of $\text{CaSO}_4 \cdot 2\text{H}_2\text{O}$ in K4 become most visible. This indicates that SG doping at 0.04% will postpone PGSL's early hydration but have minimal effect on its later hydration.

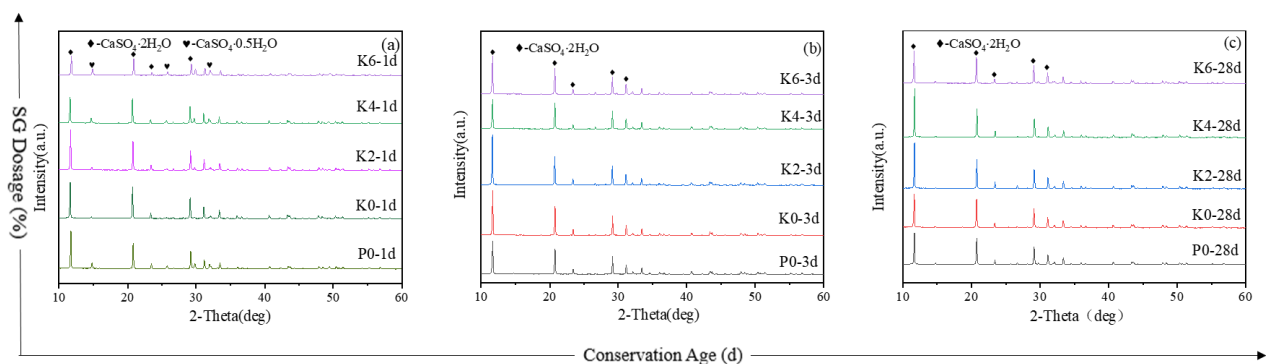


Figure 8. The XRD pattern of samples at (a) 1 d, (b) 3 d, and (c) 28 d.

3.7. Pore Structure

The physical properties of materials are closely related to their microscopic properties, and testing the pore structure is an essential means of testing the apparent microscopic properties. Generally speaking, the theoretical water requirement of $\text{CaSO}_4 \cdot 0.5\text{H}_2\text{O}$ is only 18.6% of its weight. Still, in the production process of gypsum self-leveling, the actual amount of water added is much more considerable than its theoretical water requirement, which makes the excess water retained inside the gypsum slurry and precipitated as water vapor with the hydration process of gypsum, which leads to the emergence of many pores inside the gypsum [29]. Generally, pores with pore sizes >200 nm significantly influence gypsum properties [35]. The pore structure of PGSL is seen in Figure 9. Figure 9 shows that the SG-doped PGSL has significantly fewer detrimental pores than the PR-doped one. With the inclusion of SG during compounding, the detrimental pores and overall porosity inside the PGSL were greatly reduced, presumably because the gypsum hardened more quickly. In the early stages, the entire skeletal structure is produced, and as the gypsum continues to hydrate, it solidifies. The hydration of cement is greatly slowed down by the addition of SG, which has a negative impact on the gypsum's skeleton structure and increases porosity. In conclusion, adding SG can make PGSL's pore structure smaller.

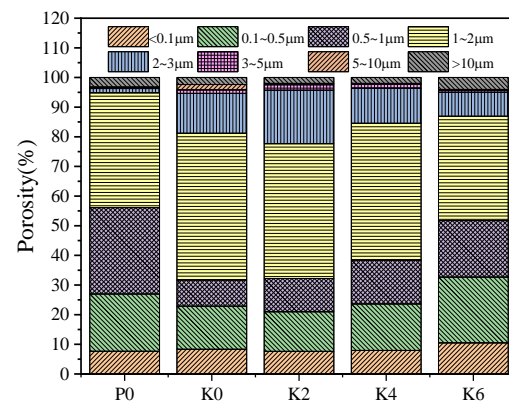


Figure 9. Pore size distribution of samples.

3.8. Micromorphology

The microscopic morphology of the PGSL samples after 1 d and 28 d of hydration is depicted in Figure 10. As seen in Figure 10a, the system's structure is still somewhat loose even after being hydrated to a level of 1d. These big plate-like crystals may represent $\text{CaSO}_4 \cdot 0.5\text{H}_2\text{O}$ crystals that are still partially hydrated. It is evident from Figure 10b that the number of these partially hydrated $\text{CaSO}_4 \cdot 0.5\text{H}_2\text{O}$ plate-like crystals increased following the addition of SG, confirming that the presence of SG delayed the hydration of $\text{CaSO}_4 \cdot 0.5\text{H}_2\text{O}$ crystals. Figure 10c,d show that after the sample was hydrated for 28 d, the addition of SG caused the sample's porosity to decrease and the crystals to become more compact.

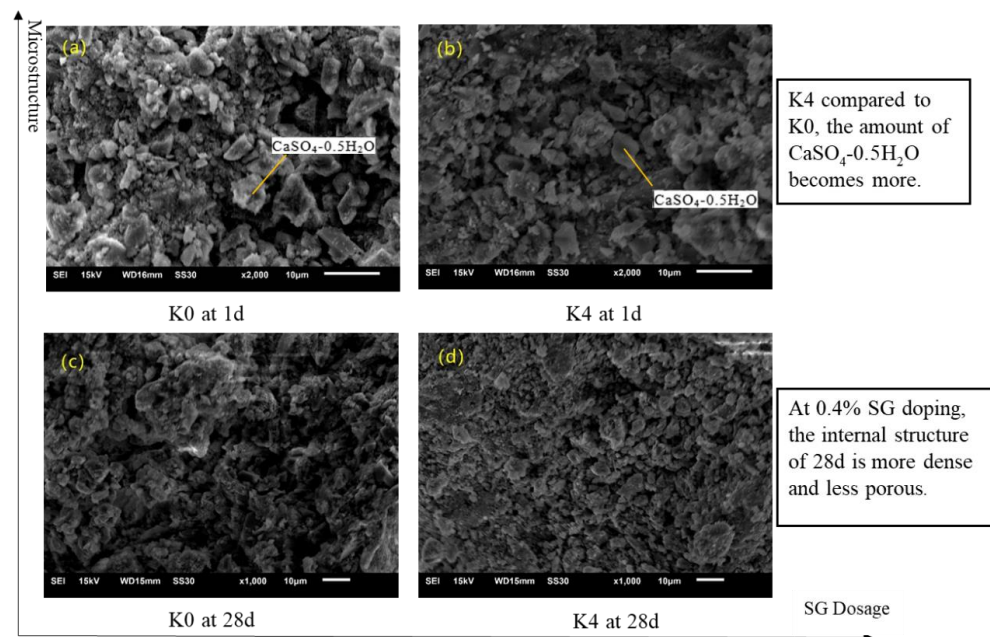


Figure 10. Effect of SG on the microscopic morphology of samples.

4. Discussion

This study examines the impact of SG and PR single and compound mixing on the gypsum's self-leveling qualities in an effort to enhance PGSL's operational performance. The following is a summary of the key findings:

- (1) $\text{CaSO}_4 \cdot 0.5\text{H}_2\text{O}$'s hydration can be postponed by SG and PR alike. When SG mixes with free calcium ions, it forms chelates that reduce the solubility of calcium ions in the solution and postpone the hydration of $\text{CaSO}_4 \cdot 0.5\text{H}_2\text{O}$. The setting time of PGSL increases nearly linearly when the SG dosage is increased when SG and PR

- are combined, and the difference between the initial and final setting durations gradually widens;
- (2) The flow loss of both SG and PR is large; when these two admixtures are compounded, the working performance is significantly improved, and when the SG addition reaches 0.06%, the flow loss is the smallest, only 2 mm. This fully meets the needs of practical use;
 - (3) When 0.04% SG and 0.03% PR are compounded, the 1 d and 3 d strengths of gypsum self-leveling will decrease, but the 28 d strength will be improved, and the flexural and compressive strengths are improved by 25.49% and 6.38%, respectively;
 - (4) The addition of SG prolongs the induction period of $\text{CaSO}_4 \cdot 0.5\text{H}_2\text{O}$ in PGSL and retards the hydration process of gypsum. In addition, it also significantly retards the hydration of C_3A , and the higher the dosage of SG, the more pronounced the retardation of hydration;
 - (5) When hydrated to 28 d, the total porosity of PGSL decreased, the average pore diameter became larger, and the microcrystalline structure was more dense when SG and PR were doped;
 - (6) The setting time was moderate, the mobility loss was 6 mm, the 1 d flexural and compressive strengths were 2.1 MPa and 8.9 MPa, and the 28 d flexural and compressive strengths were 6.4 MPa and 25 MPa when 0.04% SG and 0.03% PR were doped. The 28 d shrinkage rate was -0.03% , and all PGSL output during this period was of outstanding quality.

Author Contributions: Conceptualization, X.S.; methodology, X.S.; software, H.D.; validation, Z.C., W.A. and Y.L.; formal analysis, A.C.; investigation, Y.F.; resources, A.C.; data curation, Y.F.; writing—original draft preparation, X.S.; writing—review and editing, X.S. and D.L. (Dongyi Lei); supervision, Y.F.; project administration, D.L. (Dongyi Lei); funding acquisition, D.L. (Dongxu Li). All authors have read and agreed to the published version of the manuscript.

Funding: The National Natural Science Foundation of China (U23A20673, U22A20244), Qingdao West Coast New Area 2021 Science and Technology Plan Special Project (2021-102), Qingchuang Technology Project (2021KJ045), the Science and Technology Plan Projects of Sichuan Province (2021YFSY0002), and A Project Funded by the Priority Academic Program Development of Jiangsu Higher Education Institutions (PAPD) were jointly responsible for this work.

Data Availability Statement: Data are contained within the article.

Acknowledgments: The authors would like to thank Nanjing Kunchang new material Co. for providing the raw materials and experimental equipment.

Conflicts of Interest: Author Aili Chen was employed by the company Nanjing Kunchang New Material Co. The remaining authors declare that the research was conducted in the absence of any commercial or financial relationships that could be construed as a potential conflict of interest.

References

1. Chernysh, Y.; Yakhnenko, O.; Chubur, O.; Roubík, H. Phosphogypsum recycling: A review of environmental issues, current trends, and prospects. *Appl. Sci.* **2021**, *11*, 1575. [[CrossRef](#)]
2. Qin, X.; Cao, Y.; Guan, H.; Hu, Q.; Liu, Z.; Xu, J.; Hu, B.; Zhang, Z.; Luo, R. Resource utilization and development of phosphogypsum-based materials in civil engineering. *J. Clean. Prod.* **2023**, *387*, 135858. [[CrossRef](#)]
3. Gong, Y.; Dong, S.; Liu, L.; Wu, F. A sustainable composite cementitious material manufactured by phosphogypsum waste. *Appl. Sci.* **2022**, *12*, 12718. [[CrossRef](#)]
4. Calderón-Morales, B.R.S.; García-Martínez, A.; Pineda, P.; García-Tenório, R. Valorization of phosphogypsum in cement-based materials: Limits and potential in eco-efficient construction. *J. Build.* **2021**, *44*, 102506. [[CrossRef](#)]
5. Xue, S.; Li, M.; Jiang, J.; Millar, G.J.; Li, C.; Kong, X. Phosphogypsum stabilization of bauxite residue: Conversion of its alkaline characteristics. *J. Environ. Sci.* **2019**, *77*, 1–10. [[CrossRef](#)]
6. Chen, M.; Liu, P.; Kong, D.; Li, Y.; Chen, Y.; Cui, G.; Wang, J.; Yu, K.; Wu, N. Performance study and multi-index synergistic effect analysis of phosphogypsum-based composite cementitious material. *Coatings* **2022**, *12*, 1918. [[CrossRef](#)]
7. Li, Y.; Dai, S.; Zhang, Y.; Huang, J.; Su, Y.; Ma, B. Preparation and thermal insulation performance of cast-in-situ phosphogypsum wall. *J. Appl. Biomater.* **2018**, *16*, 81–92. [[CrossRef](#)]
8. Zhang, H.; Cheng, Y.; Yang, L.; Song, W. Modification of lime-fly ash-crushed stone with phosphogypsum for road base. *Adv. Civ. Eng.* **2020**, *2020*, 8820522. [[CrossRef](#)]

9. Zhi, Z.; Huang, J.; Guo, Y.; Lu, S.; Ma, B. Effect of chemical admixtures on setting time, fluidity and mechanical properties of phosphorus gypsum-based self-leveling mortar. *KSCE J. Civ. Eng.* **2017**, *21*, 1836–1843. [[CrossRef](#)]
10. Arulmoly, B.; Konthesingha, C.; Nanayakkara, A. Effects of blending manufactured sand and offshore sand on rheological, mechanical and durability characterization of lime-cement masonry mortar. *Eur. J. Environ.* **2021**, *26*, 7400–7426. [[CrossRef](#)]
11. Hu, W. Impacts of human activities in the hanjiang river basin, China. *J. Coast. Res.* **2019**, *96*, 68–75. [[CrossRef](#)]
12. Padmalal, D.; Maya, K.; Sreebha, S.; Sreeja, R. Environmental effects of river sand mining: A case from the river catchments of Vembanad lake, southwest coast of India. *Environ. Geol.* **2007**, *54*, 879–889. [[CrossRef](#)]
13. Yang, X.; Li, C.; Wu, J. The application of blast furnace slag in cementitious self-leveling mortar. *Adv. Mat. Res.* **2011**, 328–330, 1122–1126. [[CrossRef](#)]
14. Li, R.; He, W.; Duan, J.; Feng, S.; Zhu, Z.; Zhang, Y. Existing form and distribution of fluorine and phosphorus in phosphate rock acid-insoluble residue. *Environ. Sci. Pollut. Res.* **2022**, *29*, 7758–7771. [[CrossRef](#)] [[PubMed](#)]
15. Jiang, Y.; Kwon, K.D.; Wang, D.; Ren, C.; Li, W. Molecular speciation of phosphorus in phosphogypsum waste by solid-state nuclear magnetic resonance spectroscopy. *Sci. Total Environ.* **2019**, *696*, 133958. [[CrossRef](#)] [[PubMed](#)]
16. Zhang, J.; Wang, X.; Jin, B.; Liu, C.; Zhang, X.; Li, Z. Effect of soluble P₂O₅ form on the hydration and hardening of hemihydrate phosphogypsum. *Adv. Mater. Sci. Eng.* **2022**, *2022*, 1212649. [[CrossRef](#)]
17. Wang, Q.; Jia, R. A novel gypsum-based self-leveling mortar produced by phosphorus building gypsum. *Constr. Build. Mater.* **2019**, *226*, 11–20. [[CrossRef](#)]
18. Silva, D.B.P.; Lima, N.B.; Lima, V.M.E.; Estolano, A.M.L.; Nascimento, H.C.B.; Vilemen, P.; Padron-Hernández, E.; Carneiro, A.M.P.; Lima, N.B.D.; Povoas, Y.V. Producing a gypsum-based self-leveling mortar for subfloor modified by polycarboxylate admixture (PCE). *Constr. Build. Mater.* **2023**, *364*, 130007. [[CrossRef](#)]
19. Ma, S.; Li, W.; Zhang, S.; Ge, D.; Yu, J.; Shen, X. Influence of sodium gluconate on the performance and hydration of Portland cement. *Constr. Build. Mater.* **2015**, *91*, 138–144. [[CrossRef](#)]
20. Ren, J.; Fang, Y.; Ma, Q.; Tan, H.; Luo, S.; Liu, M.; Wang, X. Effect of storage condition on basic performance of polycarboxylate superplasticiser system incorporated sodium gluconate. *Constr. Build. Mater.* **2019**, *223*, 852–862. [[CrossRef](#)]
21. Lin, C.; Liu, Z.; Gao, Y.; Li, Z.; Zhang, J.; Niu, H. Study on the effect and mechanism of cement-based material retarder on red mud-based hybrid alkali activated cement. *J. Build.* **2023**, *70*, 106353. [[CrossRef](#)]
22. GB/T 36141-2018; Methods for Phase Composition Analysis of Calcined Gypsum. China Building Materials Industry Press: Beijing, China, 2018.
23. JC/T 1023-2021; Gypsum Based Self-Leveling Compound for Floor. China Building Materials Industry Press: Beijing, China, 2021.
24. GB/T17669.4-1999; Gypsum Pastes-Determination of Physical Properties of Pure Paste. China Building Materials Industry Press: Beijing, China, 1999.
25. GB/T17669.3-1999; Gypsum Pastes-Determination of Mechanical Properties. China Building Materials Industry Press: Beijing, China, 1999.
26. JC/T 985-2005; Cement-Based Self-Leveling Paddles for Floors. China Building Materials Academy: Beijing, China, 2005.
27. Ding, X.; Wei, B.; Deng, M.; Chen, H.; Shan, Z. Effect of protein peptides with different molecular weights on the setting and hydration process of gypsum. *Constr. Build. Mater.* **2022**, *318*, 126185. [[CrossRef](#)]
28. Tan, H.; Zou, F.; Ma, B.; Guo, Y.; Li, X.; Mei, J. Effect of competitive adsorption between sodium gluconate and polycarboxylate superplasticizer on the rheology of cement paste. *Constr. Build. Mater.* **2017**, *144*, 338–346. [[CrossRef](#)]
29. Jiao, J.; Shen, S.; Ding, H.; Lu, D.; Li, D. Study on the hydration and properties of multiphase phosphogypsum synergistically activated by sodium sulfate and calcium sulfate whisker. *Constr. Build. Mater.* **2022**, *355*, 129225. [[CrossRef](#)]
30. Hu, K.; Sun, Z. Influence of polycarboxylate superplasticizers with different functional units on the early hydration of C₃A-Gypsum. *Materials* **2019**, *12*, 1132. [[CrossRef](#)] [[PubMed](#)]
31. Tydlitát, V.; Tesárek, P.; Černý, R. Effects of the type of calorimeter and the use of plasticizers and hydrophobizers on the measured hydration heat development of FGD gypsum. *J. Therm. Anal.* **2008**, *91*, 791–796. [[CrossRef](#)]
32. Florian, A.H.; Johann, P. Impact of aging on the hydration of tricalcium aluminate(C₃A)/gypsum blends and the effectiveness of retarding admixtures. *Z. Naturforsch. B* **2020**, *75*, 739–753. [[CrossRef](#)]
33. Zhang, X.; He, Y.; Lu, C.; Huang, Z. Effects of sodium gluconate on early hydration and mortar performance of portland cement-calcium aluminate cement-anhydrite binder. *Constr. Build. Mater.* **2017**, *157*, 1065–1073. [[CrossRef](#)]
34. Zhao, H.; Sun, W.; Wu, X.; Gao, B. The properties of the self-compacting concrete with fly ash and ground granulated blast furnace slag mineral admixtures. *J. Clean. Prod.* **2015**, *95*, 66–74. [[CrossRef](#)]
35. Zhang, X.; Zhou, S.; Zhou, H.; Li, D. The effect of the modification of graphene oxide with gamma-aminopropyltriethoxysilane (KH550) on the properties and hydration of cement. *Constr. Build. Mater.* **2022**, *322*, 126497. [[CrossRef](#)]

Disclaimer/Publisher’s Note: The statements, opinions and data contained in all publications are solely those of the individual author(s) and contributor(s) and not of MDPI and/or the editor(s). MDPI and/or the editor(s) disclaim responsibility for any injury to people or property resulting from any ideas, methods, instructions or products referred to in the content.